6-1-2012

Effect of Fluxing Additive on Sintering Temperature, Microstructure and Properties of $BaTiO_3$

Yaseen Iqbal
University of Peshawar

Asad Jamal
University of Peshawar

Riaz Ullah
University of Peshawar

M. Naeem Khan
University of Peshawar

Rick Ubic
Boise State University

Bull. Mater. Sci., Vol. 35, No. 3, June 2012, pp. 387–394. © Indian Academy of Sciences.

Effect of fluxing additive on sintering temperature, microstructure and properties of $BaTiO_3$

YASEEN IQBAL*, ASAD JAMAL, RIAZ ULLAH, M NAEEM KHAN and RICK UBIC†
Materials Research Laboratory, Institute of Physics & Electronics, University of Peshawar, Peshawar 25120, Pakistan
†College of Engineering, Boise State University, Idaho, USA

MS received 15 June 2011; revised 30 July 2011

Abstract. Various fluxing materials are added to technical ceramics in an attempt to lower their sintering temperatures and make their processing economical. The effect of 0·3 wt% Li_2CO_3 addition on the phase, microstructure, phase transition temperatures and dielectric properties of $BaTiO_3$ was investigated in the present study. The addition of 0·3 wt% Li_2CO_3 was observed to lower the optimum sintering temperature by ∼200°C with no second phase formation and cause a five-fold reduction in grain size. Rhombohedral-to-orthorhombic and tetragonal-to-cubic phase transitions at the expected temperatures were evident from the Raman spectra, but the orthorhombic-to-tetragonal phase transition was not clearly discernible. The persistence of various phase(s) at higher temperatures in the flux-added materials indicated that the phase transitions occurred relatively slowly. A decrease in dielectric constant of Li_2O-added $BaTiO_3$ in comparison to pure $BaTiO_3$ may be due to the diminished dielectric polarizability of Li^+ in comparison to Ba^{2+}.

Keywords. Electronic materials; Raman spectroscopy; dielectric properties; microstructure.

1. Introduction

Barium meta-titanate ($BaTiO_3$) is widely used in electronic devices, such as multilayer ceramic capacitors (MLCCs), tunable filters and piezoelectric sensors due to its high chemical and mechanical stability, ferroelectric properties at and above room temperature, easy preparation methods and high dielectric constant (Wul 1945; Bunting *et al* 1947). It is also used in positive temperature coefficient resistors (PTCR) such as thermistors, electroluminescent panels and pyroelectric elements. Its global production is $\sim 11 \times 10^6$ kg/annum and the MLCC industry alone is a multi-billion dollar industry in which more than 10 billion units are produced annually (O'Bryan and Thomson 1974; Scott 1993; Swartz and Shrout 1997; Bell 2008).

$BaTiO_3$ was discovered in 1839 and became the first useful ferroelectric material with a perovskite-type structure (Wul 1945). An early example of an application of $BaTiO_3$ was the unprecedented achievement of high specific capacitance made possible by the modification of $BaTiO_3$ with isovalent substitutions (e.g. Sr^{2+}) in order to shift the Curie temperature (T_C) closer to room temperature (Jaffe and Cook 1971; Scott 1993). From the late 1940s, efforts have been underway to produce highly homogeneous, fully dense, multi-component oxides to tailor dielectric properties for commercial use (Batllo *et al* 1990; Heartling 1999; Langhammaer *et al* 2000; Masion *et al* 2003; Millsch 2006). The classic BaO–TiO_2 phase equilibrium diagram of Rase and Roy (O'Bryan and Thomson 1974) shows the presence of a 1317°C eutectic close to the $BaTi_2O_5$ composition which was later identified as $Ba_6Ti_{17}O_{40}$.

$BaTiO_3$ is a ferroelectric ceramic material with a perovskite structure. It has four polymorphs, viz. rhombohedral, orthorhombic, tetragonal and cubic. There is also an hexagonal form which is stable above ∼1430°C. The tetragonal form of $BaTiO_3$ is stable at room temperature, whereas the cubic form is stable at high temperatures (>120°C). All forms have a relatively high dielectric constant (Pasha *et al* 2007). Cubic $BaTiO_3$ has one dielectric constant denoted by ε_r whereas the dielectric constant of tetragonal $BaTiO_3$ consists of two components, denoted by ε_a and ε_c, corresponding to directions perpendicular and parallel to the polar axis. At room temperature, the numerical value of its spontaneous polarization is 26×10^{-2}C/cm^2.

Most of the commercial electroceramics compositions are modified via doping in one way or another; and processing, phase and microstructural studies of some basic compositions leading to their improved densification and properties accompanied by lowering of the sintering temperature are always sought. Such studies have been crucial in pointing the way towards modern dielectric formulations. For example, $BaTiO_3$-based ceramics with a 1 μm grain size have been produced via fast-firing with a three-fold increase in permittivity over the coarse-grained material. Anan'eva *et al* (1960) reported an almost six-fold increase in permittivity by similar techniques. The origin of this anomalous effect is still under discussion over 50 years later. This continuous struggle has

*Author for correspondence (dryaseeniqbal@yahoo.co.uk)

not just been a scientific curiosity but has lead to the development of modern capacitor dielectrics. The exploitation of this effect in X7R dielectric materials required an in-depth understanding of chemistry. It is now known that donor dopants inhibit grain growth, providing a means of exploiting the anomalous grain size effect without exotic thermal processing; however, donor doping also affects electrical conductivity in $BaTiO_3$ (Anan'eva *et al* 1960; Desu and Subbarao 1981; Manczok and Wernicke 1983; Wang 2002; Masion *et al* 2003); therefore, a thorough understanding of the compensation mechanism by acceptor additions is required (Galasso 1996).

The effect of various fluxing additives on the phase, microstructure and properties of $BaTiO_3$ are constantly investigated in an attempt to lower its sintering temperature and reduce processing cost; but such additions result in the formation of second phases or pores, leading to deterioration of properties. For example, the addition of 3 mol% BaB_2O_4 to sol–gel-derived semiconducting Y-doped $BaTiO_3$ has been reported to lower its sintering temperature to 1050°C; however, BaB_2O_4 not only forms a non-conductive amorphous phase, but the volatilization of a boron-rich liquid phase leads to the formation of pores which adversely affect the density of ceramics (Kong *et al* 2009). Similarly, the addition of >5 wt% of the 60·7 ZnO–24·9 B_2O_3–14·4 SiO_2 (mol%) glass has been reported to enable the sintering of $BaTiO_3$ to 95% of theoretical density at temperatures as low as 900°C without the formation of a second phase, but with a dielectric constant of only 994 (Hsiang *et al* 2009).

The addition of small amounts of Li_2O to various ceramic compositions has been reported to lower the sintering temperature by various mechanisms. In aluminium nitride (AlN), the addition of Li_2O has been observed to densify the material at a lower temperature (∼1650°C) than pure AlN (sintering temperature > 1800°C) due to the formation of a Li-containing liquid phase at ∼1100°C. Additionally, the volatilization of a Li-containing phase at high temperatures purifies the grain boundaries of the parent material (Qiao *et al* 2003). Similarly, Li_2CO_3 addition to $SrTiO_3$, has also been observed to lower its sintering temperature but simultaneously form Li-containing second phase(s) which could be eliminated either by controlling the amount of Li_2CO_3 added or sintering the ceramic at a high temperature to eliminate the volatile Li-containing phase (Cheng *et al* 1989). The addition of Li_2CO_3 to $BaTiO_3$–Nb_2O_5–La_2O_3–Sm_2O_3 has been reported to improve the dielectric constant at temperatures near the Curie temperature (Li *et al* 2001). The addition of 0·3 wt% Li_2O in the form of polycrystalline Li_2O, Li_2CO_3 or as an ascetic solution of Li^+ ions to $BaTiO_3$ has been observed to lower its sintering temperature by ∼400°C (from ∼1250°C to 820°C), independent of the form of Li_2O added. It has been reported that Li_2O and $BaTiO_3$ first reacted to form $BaCO_3$ and Li_2TiO_3 at 600°C. These pre-reacted powders when milled and compacted, sinter to >95% of the relevant theoretical density at 820°C, but result in the retention of Li_2TiO_3 and Ba_2TiO_4 in small concentrations (Valant *et al* 2006).

In this study, results regarding the phase, microstructure and dielectric properties of $BaTiO_3$ prepared via a mixed-oxide route and a reactive-phase sintering route via donor doping have been described and discussed. Additionally, *in situ* Raman spectroscopy has been used for the first time to investigate and compare the phase transition temperatures of pure and Li_2CO_3-added $BaTiO_3$.

2. Experimental

Batches (50 g) of GPR grade TiO_2 and $BaCO_3$ (Aldrich Chemicals Company Inc.) powder were prepared and mix-milled for 24 h in a horizontal ball mill with Y-PSZ balls as milling media and 2-propanol as lubricant. The resulting slurry was poured through a sieve into a glass beaker and dried at ∼90°C overnight. After sieving, the resulting powder samples were calcined at 900°C for 2 h, with a heating/cooling rate of 10°C/min. The calcined powders were re-milled for 30 min to dissociate agglomerates, dried, sieved and pressed into 13 mm diameter pellets at 100 MPa. The pellets were sintered at 1250°C for 2 h with a heating/cooling

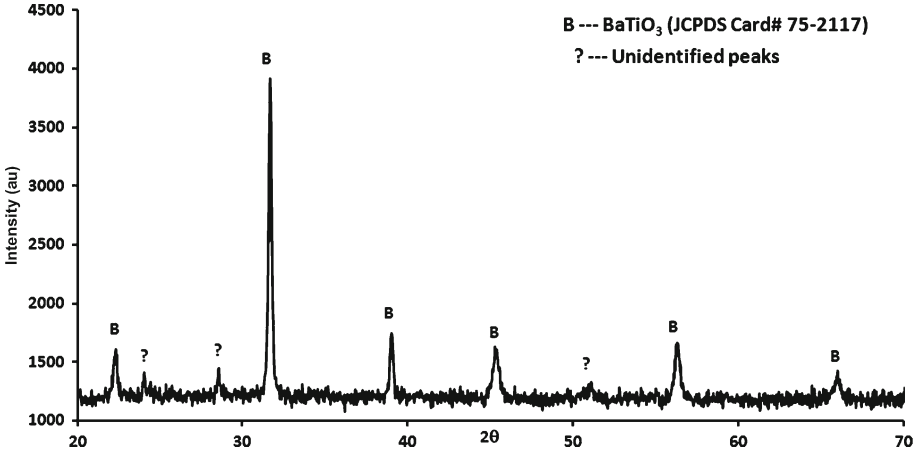

Figure 1. X-ray diffractogram of $BaTiO_3$ calcined at 900°C showing the formation of tetragonal $BaTiO_3$ phase along with a couple of low intensity peaks, showing incomplete reaction.

rate of 5°C/min. The reactive-phase sintering route was the same as the mixed-oxide route except that 0·3 wt% Li_2CO_3 sintering aid was added and milled-in after calcination. The phase analysis of the samples was carried out using an X-ray diffractometer (XRD) (1700 series, Philips, The Netherlands) with CuKα radiation operating at 40 kV and 30 mA with a step size of 0·02° from 10 to 70° at 1°/min. For microstructural characterization a scanning electron microscope (SEM) (JSM-5910, JEOL, Japan) operating at 15–20 kV was used. The sintered samples were cut into two pieces by a fine diamond wafering blade before fine polishing. The samples were thermally etched at temperatures ~10% lower than the relevant sintering temperatures at 5°C/min for 30 min to resolve the grains. To provide a conducting medium and avoid charging in the SEM, the samples were mounted on metallic stubs with silver paint and gold-coated. Electrical properties of pellets were measured using an LCR meter (model 4287A, HP, USA) from *RT*–300°C at 1 kHz–1 MHz. Density of the sintered samples was measured using an electronic densitometer (MD-300S, Lako Tool and Manufacturing Inc, Ohio, USA). *In situ* Raman spectroscopy was performed to determine and compare the phase transition temperatures using a micro-Raman spectrometer (Renishaw InVia) with 514·5 nm line of Ar-laser in the 100–1000 cm^{-1} range at 5°C interval from −190 to 300°C.

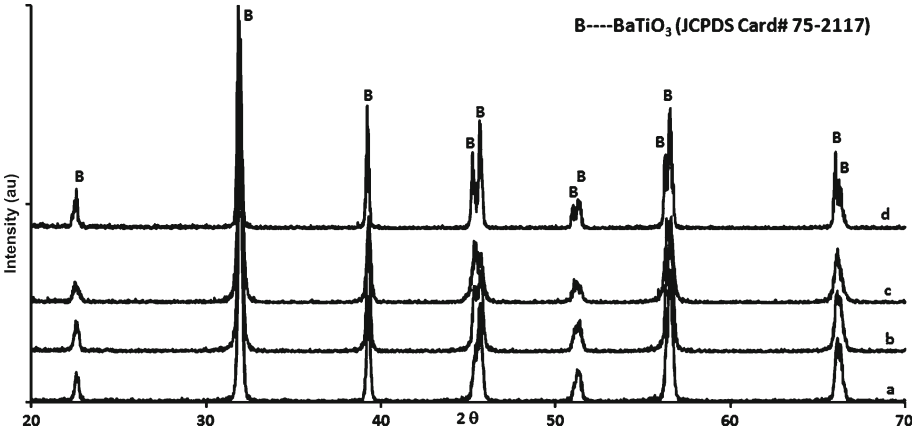

Figure 2. X-ray diffractogram of Li_2CO_3-added $BaTiO_3$ calcined at 900°C and sintered at (**a**) 1000°C, (**b**) 1050°C and (**c**) 1100°C showing formation of tetragonal $BaTiO_3$ phase only. (**d**) is from pure $BaTiO_3$ sample, calcined at 900°C and sintered at 1250°C.

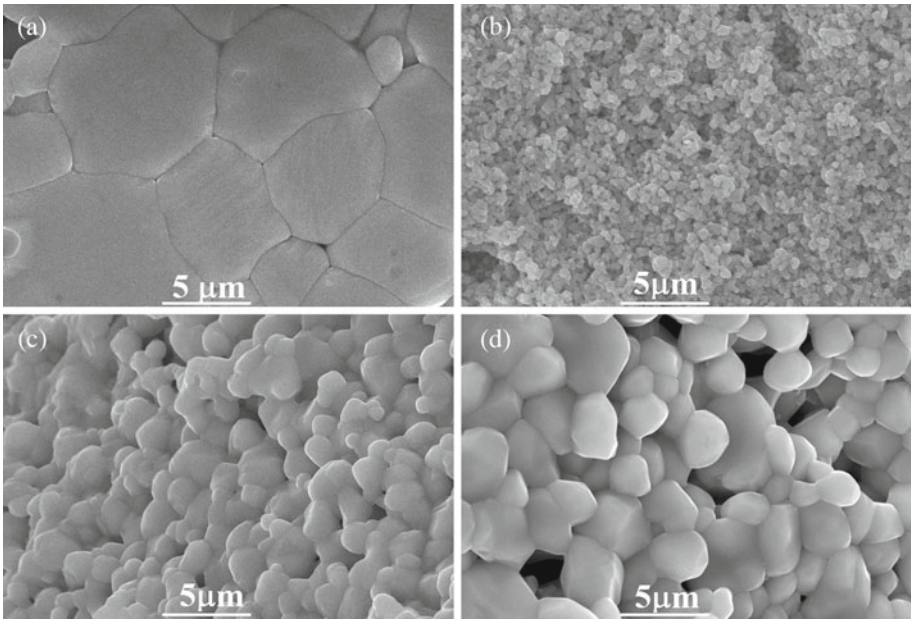

Figure 3. SEI from (**a**) pure $BaTiO_3$ sample calcined at 900°C and sintered at 1250°C for 2 h showing ~2 to 10 μm $BaTiO_3$ grains, (**b**) 0·3 wt% Li_2CO_3-added $BaTiO_3$ sample, calcined at 900°C, showing ≤0·5 μm grains in sample sintered at 1000°C, (**c**) 1–1·5 μm grains in sample sintered at 1050°C and (**d**) 1–2 μm grains in sample sintered at 1100°C.

3. Results and discussion

Tetragonal $BaTiO_3$ (PDF# 75–2117) was the major phase identified by XRD in the sample calcined at 900°C; however, the presence of a couple of low-intensity XRD peaks labelled as '?' which could not be identified were indicated as incomplete reaction at the calcination temperature (figure 1). All the inter-planar spacings (d-values) and relevant intensities of XRD peaks from the sample calcined at 900°C and sintered at 1250°C matched with PDF# 75–2117 for tetragonal $BaTiO_3$ (figure 2d). The absence of extra peaks in this XRD pattern confirmed phase purity of the final ceramics. The d-values corresponding to XRD peaks from 0·3 wt% Li_2CO_3 added samples calcined at 900°C and sintered at 1000°C, 1050°C and 1100°C also matched with PDF# 75–2117 for tetragonal $BaTiO_3$ (figures 2a–c). The asymmetry of the peaks at 2θ ~45·5°, 51°, 56·5° and 66° corresponding to (2 0 0), (2 0 1), (2 1 1) and (2 2 0) planes for

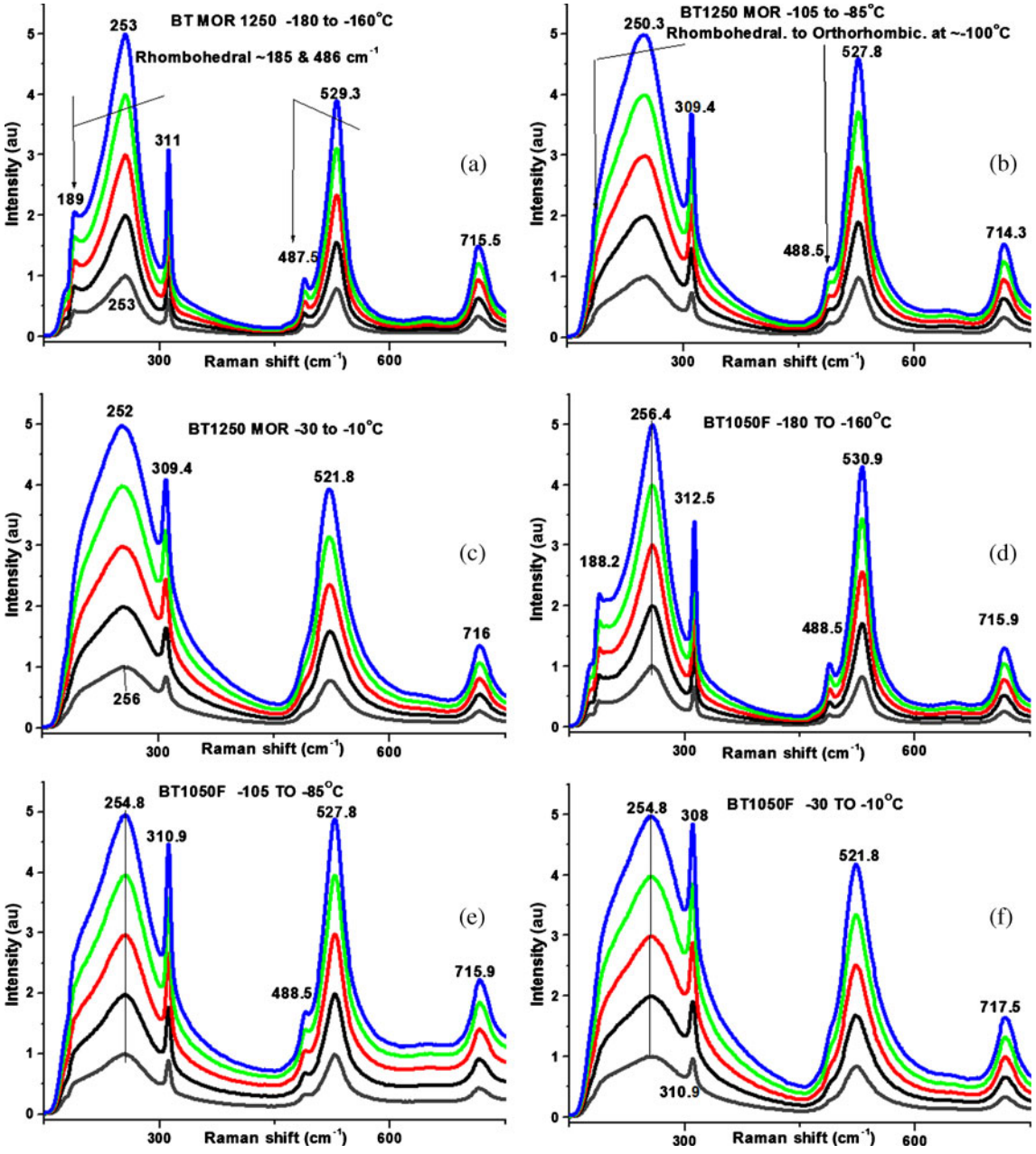

Figure 4. Raman spectra from pure $BaTiO_3$ sample collected at (**a**) −180 to −160°C, (**b**) −105 to −85°C and (**c**) −30 to −10°C, and Li_2CO_3-added samples at (**d**) −180 to −160°C, (**e**) −105 to −85°C and (**f**) −30 to −10°C. Note the presence of peaks at ~189 and 487 cm^{-1} indicative of rhombohedral phase collected at −180 to −160°C (figures (**a**) and (**d**)) and their partial disappearance at −105 to −85°C (figures (**b**) and (**e**)) and disappearance at −30 to −10°C (figures (**c**) and (**f**)).

samples sintered at 1000–1100°C indicated that all the peaks visible at 1250°C were present but were too broad to be clearly resolved due to small crystal size. It is noticeable that no extra XRD peaks due to second phase(s) or remnant starting powders due to incomplete reaction could be observed on any of these XRD patterns, demonstrating the phase-purity of the final ceramics within the detection limits of XRD in the present study. The previously reported presence of small amounts of Li_2TiO_3 and Ba_2TiO_4 in 0·3 wt% Li_2CO_3-added $BaTiO_3$ sintered at 820°C may be due to the much lower sintering temperature, indicative of incomplete reaction (Valant *et al* 2006).

Secondary electron SEM images (SEI) from the $BaTiO_3$ samples prepared via the mixed-oxide route calcined at 900°C and sintered at 1250°C for 2 h show grain sizes from ~2 to 10 μm (figure 3a). Contrastingly, pure $BaTiO_3$ samples heated at temperatures $\leq$1100°C were not dense and could be scratched with a finger nail. On the other hand,

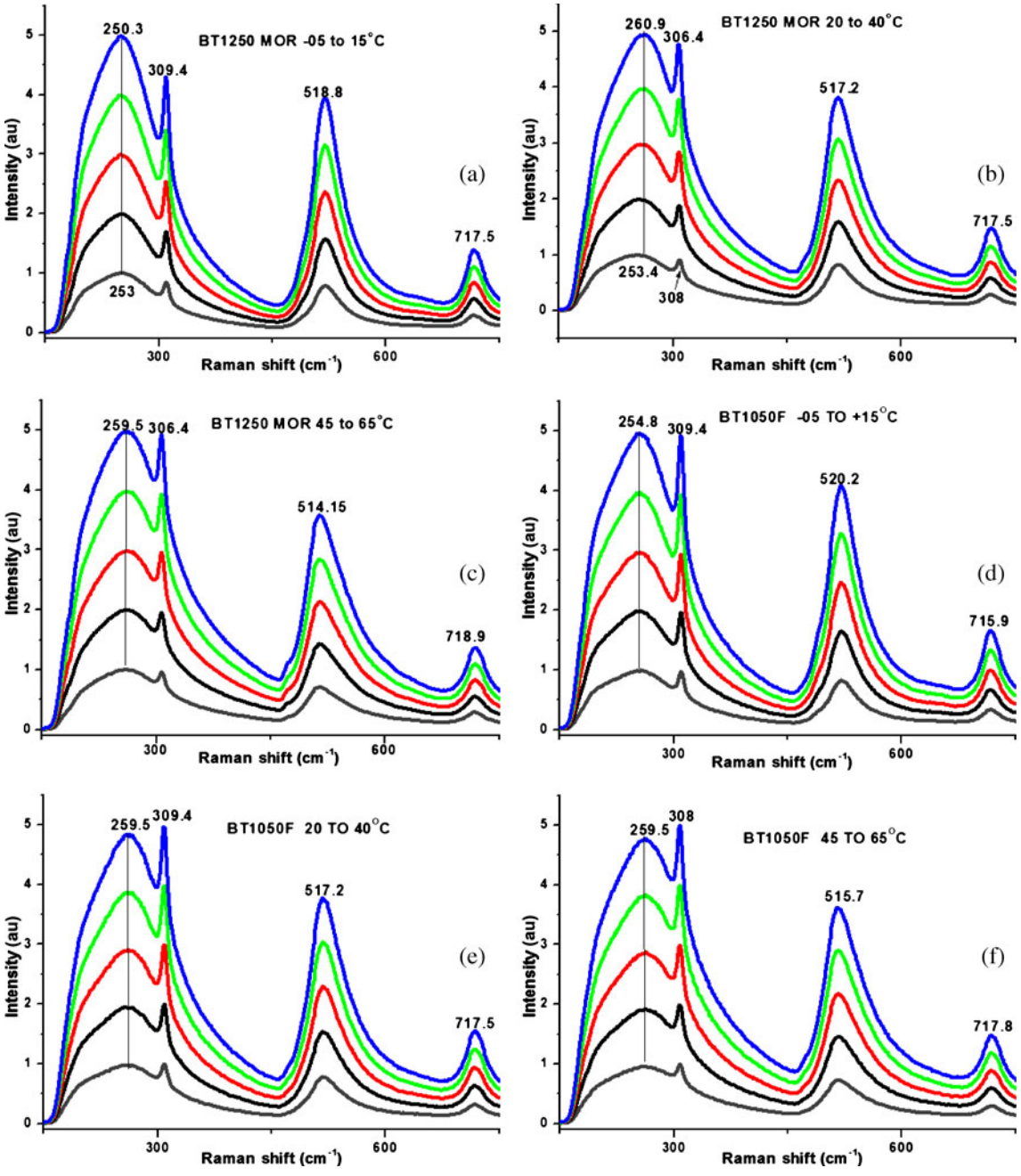

Figure 5. Raman spectra from pure $BaTiO_3$ samples collected at (**a**) −5 to +15°C, (**b**) 20–40°C and (**c**) 45–65°C, and Li_2CO_3-added samples at (**d**) −5 to +15°C, (**e**) 20–40°C and (**f**) 45–65°C. Note the asymmetry of the peak at ~518·8 cm^{-1} and at ~10°C, indicative of orthorhombic-to-tetragonal phase transition (Galasso 1996); however, a careful examination shows that this asymmetry is visible even at temperatures above and below 10°C.

the deformation of Li_2CO_3-added samples showed the beginning of melting upon sintering at temperatures >1100°C. The maximum density of pure $BaTiO_3$ measured in this study was 4·75 g/cm^3. The density of Li_2CO_3-added $BaTiO_3$ varied from 4·20 to 4·73 g/cm^3 with increase in the sintering temperature from 1000 to 1050°C, which demonstrated ∼200°C decrease in the sintering temperature in comparison to pure $BaTiO_3$. Upon further increase in the sintering temperature to 1100°C, the density decreased to 4·5 g/cm^3.

The microstructure of 0·3 wt% Li_2CO_3-added $BaTiO_3$ sample calcined at 900°C and fired at 1000°C comprised ≤0·5 μm grains (figure 3b). This sample did not appear dense visually; however, the observed light necking of the grains

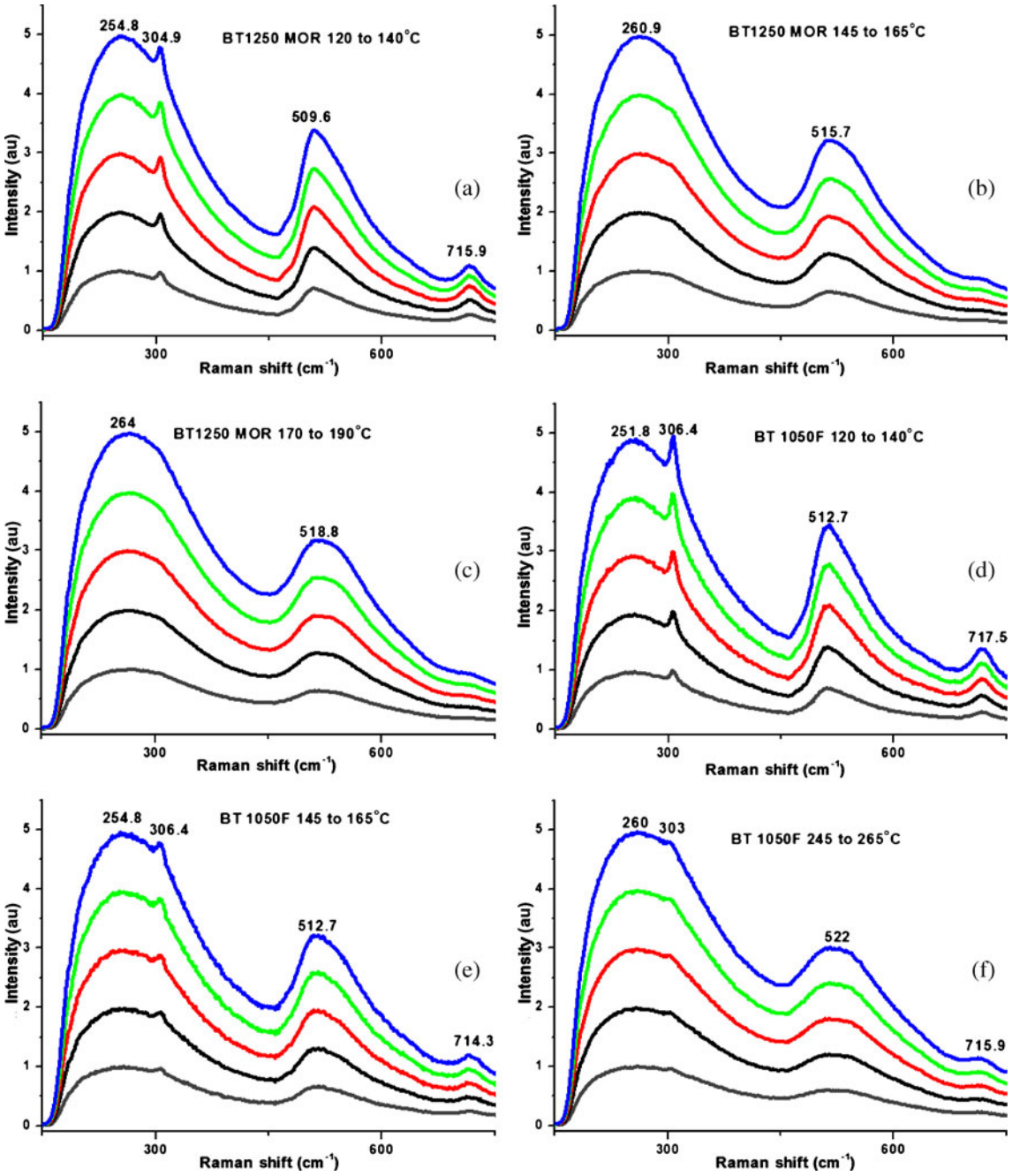

Figure 6. Raman spectra from pure $BaTiO_3$ samples collected at (**a**) 120–140°C, (**b**) 145–165°C and (**c**) 170–190°C, and Li_2CO_3-added samples at (**d**) 120–140°C, (**e**) 145–165°C and (**f**) 245–265°C. Note the presence (figures (**a**) and (**d**)) and disappearance (figures (**b**) and (**e**)) of Raman peaks at ∼305 and 306 cm^{-1} indicative of tetragonal-to-cubic phase transition at ∼124°C. Note the presence of a small peak at 303 cm^{-1} till 220°C on spectra from Li_2CO_3 containing samples and not from pure $BaTiO_3$ samples, showing relatively slower phase transition in flux-added samples.

and disappearance of sharp edges of the grains indicated the beginning of densification (figure 3b).

As shown in figure 3(c), the grain size increased from ∼1 to 1·5 μm upon increasing the sintering temperature to 1050°C, indicating more than 5-fold decrease in the grain size of $BaTiO_3$. Similarly, upon further increasing the sintering temperature to 1100°C, the grain size continued to increase up to ∼2 μm. The grain size in dense pure $BaTiO_3$ sample (sintered at 1250°C) varied from 5 to 10 μm and that of the Li_2CO_3-added samples varied from ≤1 to ≤2 μm (at 1050 and 1100°C) which indicated that the addition of Li_2CO_3 not only decreased the sintering temperature associated with the maximum density achieved in this study by ∼150°C but the grain size also decreased by about 80% in comparison to pure $BaTiO_3$ samples.

The disappearance of peaks at ∼189 and 487 cm^{-1} in the Raman spectrum of pure $BaTiO_3$ samples sintered at 1250°C indicated the transition of rhombohedral-to-orthorhombic phase at about −100°C (figures 4a–c) which is consistent with previous studies (Pasha *et al* 2007). Similarly, in Li_2CO_3-added samples sintered at 1050°C, these peaks disappeared at slightly higher temperatures, indicting slow phase transition in Li_2CO_3-containing samples (figures 4d–f). The asymmetry of the peak at 512 cm^{-1} and at ∼10°C was considered to be indicative of orthorhombic-to-tetragonal phase transition (Pasha *et al* 2007); however, in the present study, the asymmetry of the peak at ∼520 cm^{-1} could be observed not only at ∼10°C but at temperatures below and above 10°C as well (figures 5a–f) which may be due to gradual orthorhombic-to-tetragonal phase transition. The disappearance of the Raman peak at ∼308 cm^{-1} indicated the transition from the tetragonal to the cubic phase at ∼124°C (figures 6a–c). Unlike the case for pure $BaTiO_3$, a small peak at ∼308 cm^{-1} was visible up to 220°C in the spectra of Li_2CO_3-containing samples (figures 6d–f). For undoped $BaTiO_3$, Pasha *et al* (2007) reported the presence of modes at 303 and 710 cm^{-1} at temperatures above T_c which persisted at temperatures even above 180°C.

For pure $BaTiO_3$, the highest value of dielectric constant was ∼1500 at 127°C measured at 1 kHz–1 MHz (figure 7a), whereas for the Li_2CO_3-added samples it was 450 at 124°C in the same frequency range (figure 7b). The decrease in ε_r may be due to the diminished dielectric polarizability of Li^+ (1·20Å^3) compared to Ba^{2+} (6·40Å^3) (Shannon 1993). The

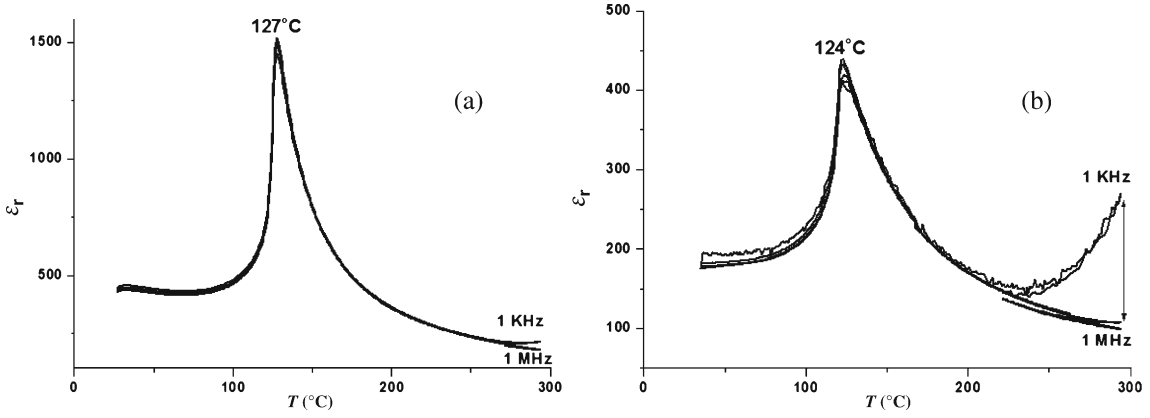

Figure 7. Variation in relative permittivity with temperature for (**a**) pure $BaTiO_3$ sintered at 1250°C and (**b**) Li_2CO_3-added $BaTiO_3$ sintered at 1050°C.

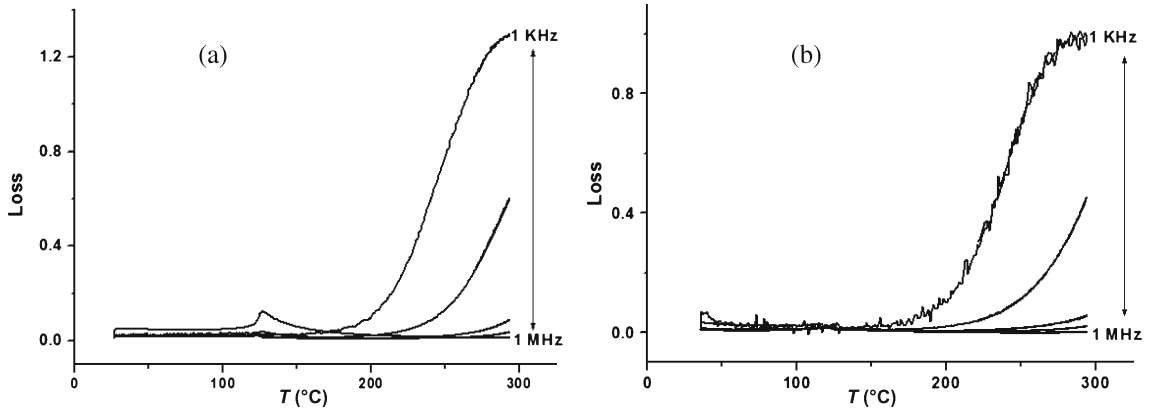

Figure 8. Variation in loss tangent with temperature for (**a**) pure $BaTiO_3$ sintered at 1250°C and (**b**) Li_2CO_3-added $BaTiO_3$ sample sintered at 1050°C.

observed T_c (127°C for pure and 124°C for $LiCO_3$-added $BaTiO_3$) for both compositions is consistent with previous studies (Galasso 1996). The maximum loss tangent values were ∼0·035 (at 1 kHz) to 0·007 (at 1 MHz) up to ∼175°C, but increased on further increase in temperature (figure 8).

4. Conclusions

The fabrication of $BaTiO_3$ via reactive liquid phase sintering has the potential to enhance the density of parts at relatively low temperatures as compared to the mixed-oxide route. Additions of 0·3 wt% Li_2CO_3 as a fluxing agent/sintering aid significantly reduced the optimal sintering temperature by ∼200°C and reduced the grain size from ≥2–10 μm to ≤1–1·5 μm. The phase transitions in the flux-added samples occurred relatively slowly in comparison to the pure samples. In contrast to previous studies of flux-added $BaTiO_3$, the final ceramic was single phase in the present study.

Acknowledgements

The authors acknowledge the financial support of the Higher Education of Pakistan via NRPU Project No. 20-569 and Development of Materials Connection Project, the US National Academy of Sciences under the Pak US S&T Cooperation Program, Award No. PGA-P280420, and Prof. I M Reaney for facilitating one of the authors in electrical properties measurement.

References

Anan'eva A A, Strizkov B W and Ugryumova M A 1960 *Bull. Acad. Sci. USSR Phys. Ser.* **24** 1395

Batllo F, Duverger E, Jules J C, Claudeniepec J, Jannot B and Maglione M 1990 *Ferroelectrics* **109** 113

Bell A J 2008 *J. Euro. Ceram. Soc.* **28** 1307

Bunting E N, Shelton G R and Creamer A S 1947 *J. Am. Ceram. Soc.* **30** 114

Cheng S, Fu S and Wei C 1989 *Ceram. Int.* **15** 231

Desu S B and Subbarao E C 1981 *Ferroelectrics* **37** 665

Galasso F S 1996 *Structure, properties and preparation of perovskite-type compounds* (Oxford: Pergamon Press)

Heartling G H 1999 *J. Am. Ceram. Soc.* **82** 797

Hsiang H, Hsi C, Huang C and Fu S 2009 *Mater. Chem. Phys.* **113** 658

Jaffe B and Cook W R 1971 *Piezoelectric ceramics* (London: Academic Press)

Kong M, Jiang S, Xie T and Zhang H 2009 *Microelec. Eng.* **86** 2320

Langhammaer H T, Muller T, Felgner K H and Abicht H P 2000 *J. Am. Ceram. Soc.* **83** 605

Li Q, Qi J, Wang Y, Gui Z and Li L 2001 *J. Eur. Ceram. Soc.* **21** 2217

Manczok R and Wernicke R 1983 *Philips Tech. Rev.* **41** 338

Masion W R, Kleeberg R, Heimann R B and Phanicphant S 2003 *J. Eur. Ceram. Soc.* **23** 127

Millsch B 2006 *Phys. Status Solidi (a)* **133** 455

O'Bryan Jr. H M and Thomson Jr. J 1974 *J. Am. Ceram. Soc.* **57** 522

Pasha U M, Zheng H, Thakur O P, Feteira A, Whittle K R, Sinclair D C and Reaney I M 2007 *Appl. Phys. Lett.* **91** 062908

Qiao L, Zhou H, Chen K and Fu R 2003 *J. Eur. Ceram. Soc.* **23** 1517

Scott A W 1993 *Understanding microwaves* (New York: John Wiley & Sons)

Shannon R D 1993 *J. Appl. Phys.* **73** 348

Swartz S L and Shrout T R 1997 *J. Am. Ceram Soc. Bull.* **76** 59

Valant M, Suvorov D, Pullar R C, Sarma K and Alford N M 2006 *J. Eur. Ceram. Soc.* **26** 2777

Wang L H 2002 *Structure and dielectric properties of perovskite-barium titanate* ($BaTiO_3$) (Peshawar: San Jose State University)

Wul B 1945 *Nature* **156** 480